# *TagBreathe*: Monitor Breathing with Commodity RFID Systems

Yanwen Wang and Yuanqing Zheng, *Member, IEEE*

**Abstract**—Breath monitoring helps assess the general personal health and gives clues to chronic diseases. Yet, current breath monitoring technologies are inconvenient and intrusive. For instance, typical breath monitoring devices need to attach nasal probes or chest bands to users. Wireless sensing technologies have been applied to monitor breathing using radio waves without physical contact. Those wireless sensing technologies however require customized radios which are not readily available. More importantly, due to interference, such technologies do not work well with multiple users. When multiple users are present, the detection accuracy of existing systems decreases dramatically. In this paper, we propose to monitor users' breathing using commercial-off-the-shelf (COTS) RFID systems. In our system, passive lightweight RFID tags are attached to users' clothes and backscatter radio waves, and commodity RFID readers report low level data (e.g., phase values). We reliably detect the effective human respiration corresponded signal and track periodic body movement due to inhaling and exhaling by analyzing the low level data reported by commodity readers. To enhance the measurement robustness, we synthesize data streams from an array of multiple tags to improve the monitoring accuracy. Our design follows the standard EPC protocol which arbitrates collisions in the presence of multiple tags. We implement a prototype for the breath monitoring system with commodity RFID systems. The experiment results show that the prototype system can simultaneously monitor breathing with high accuracy even with the presence of multiple users.

**Index Terms**—Breath monitoring, RFID, Signal phase and backscatter signal

✦

## 1 INTRODUCTION

RECENT years have witnessed the surge of mobile and wearable sensing devices and their applications in health monitoring. Breath monitoring assesses the general personal health, gives clues to chronic diseases, and tracks the progress toward recovery [5]. Scientific studies show that a deep breath reduces blood pressure and stress, while shallow breath and unconscious hold of breath indicate chronic stress [6]. People may have irregular breathing patterns alternating between fast and slow with occasional pauses [7]. As such, a convenient non-intrusive breath monitoring system would be helpful and enable innovative healthcare applications.

Current breath monitoring technologies however are inconvenient and intrusive. For instance, breath monitoring devices typically require the person to attach a nasal probe or wear chest bands [9]. Such monitoring devices restrict body movements and cause inconvenience. As such, people may feel uncomfortable to wear nasal probes or forget to wear chest bands. Parents are concerned about the safety of breath monitoring devices for their newborns. Although sensor embedded wearable devices (e.g., smart watches) can monitor some vital signs (e.g., heart rate), they cannot accurately monitor breathing.

Recent wireless sensing technologies explore the possibility of capturing vital signs (e.g., breathing patterns) using wireless signals [9], [13], [17]. Such technologies transmit wireless signals to a subject and capture periodic changes in reflected radio waves caused by chest motion during inhaling and exhaling. Those systems however require customized Doppler radios which are not readily available on the market [9]. Other systems use commodity-off-the-shelf WiFi card to measure CSI and implement respiration monitoring system. In practice, it is hard to implement such systems and reliably measure respiration due to noise and interference in the WiFi band. More importantly, when multiple users are in the presence, the reflected radio waves from the users may cause interferences and dramatically decrease monitoring accuracy. Even when monitoring a single subject, as different parts of the body simultaneously reflect radio waves, it remains challenging to accurately monitor the user's breathing patterns.

We ask the following question: *Can we use COTS systems to simultaneously monitor breathing of multiple users?* In this paper, we leverage COTS RFID systems to implement a breath monitoring system named *TagBreathe* to accurately monitor breathing even in the presence of multiple users. The *TagBreathe* system consists of several passive commodity RFID tags which are attached on users' clothes and a commodity RFID reader which captures the reflected radio waves from the tags. Researchers have embedded RFID chips into yarns which can be woven and knitted to make fabrics for RFID clothing [8], [25]. Unlike traditional battery-powered sensor motes, once attached to or embedded into cloths, the light thin RFID tags are hardly intrusive to users.

Due to chest motion during breathing, the distance between the tags to the reader varies periodically. When an user inhales the distance decreases while when the user exhales the distance increases. Such miniature variations in

• *The authors are with the Department of Computing, The Hong Kong Polytechnic University, Kowloon, Hong Kong.*
*E-mail: yanwen.wang@connect.polyu.hk, csyqzheng@comp.polyu.edu.hk.*

distance translate into small changes in data streams of low level information (e.g., phase values) reported by the reader. *TagBreathe* aggregates the low level information and extracts periodic patterns from the data stream. Compatible with the standard EPC protocol, *TagBreathe* benefits from the collision arbitration and naturally avoids interferences of multiple backscatter tags [4].

Implementing *TagBreathe* however entails substantial challenges. Based on careful characterization of low level data reported by commodity readers, we first preprocess the streams of the collected phase values. Due to frequency hopping, the phase values dramatically change when the reader hops to next frequency channels. Instead of directly tracking body movements with the raw phase values, we calculate the displacement during two consecutive phase readings measured in the same frequency channel and continuously track the body movements with the displacement values. We then carry out frequency domain analysis and extract rhythmic breathing signals from the displacement values. To better extract weak breathing signals, we further form an array of multiple tags and fuse the displacement values reported by multiple tags to improve the monitoring performance. In addition, we design an effective segmentation method to identify displacement values which are dominated by human respiration to mitigate the monitoring error.

We consolidate the above techniques and implement *Tag-Breathe* with COTS RFID systems. We evaluate *TagBreathe* in different scenarios under various experiment parameter settings. The experiment results show that *TagBreathe* is able to simultaneously monitor breathing of multiple users with high accuracies. In particular, *TagBreathe* can achieve a high breathing rate detection accuracy of less than 1 breath per minute error on average for various breathing rates.

The contribution of this paper can be summarized as follows. First, we propose a holistic design and implementation of a low cost, non-intrusive and convenient system that is able to detect breathing of multiple persons. To the best of our knowledge, *TagBreathe* is the first system that using RFID to detect human respiration and support multiple users. Second, we design and implement signal extraction algorithms to measure the breathing signals based on careful characterization of the low level data reported by a COTS RFID reader. Third, we extensively evaluate the *TagBreathe* system under various practical scenarios and demonstrate the feasibility of monitoring breathing wirelessly using COTS RFID systems.

The rest of this paper is organized as follows. We briefly describe the background of breath monitoring and COTS RFID systems in Section 2. We present the overview of *Tag-Breathe* in Section 3. We give a detailed description of key technical components of *TagBreathe* in Section 4. We present the implementation in Section 5 and the performance evaluation Section 6, respectively. Related works are summarized in Section 7. Section 8 concludes this paper.

## 2 BACKGROUND

### 2.1 Breath Monitoring System

Breath monitoring systems typically require users to attach nasal probes or wear chest bands [9]. For instance, capnometers [24] need to attach nasal cannula to patients to monitor their breathing [10]. Wearable devices (e.g., smart watches) are equipped with sensors but cannot accurately monitor breathing patterns [9], [18]. Recent wireless sensing technologies have explored the feasibility of extracting breathing patterns by measuring the reflected wireless signals from human bodies [9], [13], [17]. Such technologies transmit wireless signals to a human subject and capture the changes in the reflected radio waves due to breathing. By increasing sampling rates, recent work improves the detection resolution. To detect the small chest movements, such systems need GHz sampling rate which incurs high manufacturing cost. Instead, Doppler radios send linearly increasing frequencies and measure the frequency shift due to distance variation [9]. Those systems however require customized Doppler radios which are not readily available. More importantly, such monitoring systems may fail in the presence of multiple users, since reflected radio signals from different users mix in the air and interfere with each other. As a result, previous wireless sensing systems can only monitor one user and perform poorly with multiple human subjects.

### 2.2 RFID Sensing

Recent years have witnessed the development of accurate localization and tracking with COTS RFID systems [42]. Unlike the traditional signal strength based localization schemes [26], [40], recent schemes track the location of RFID tags based on the low level phase values of backscattered radio waves. COTS RFID readers measure low level information at RFID physical layer and output phase values for each identified tag. Although the phase measurements are subject to noises, high resolution and high sampling rate of COTS RFID systems provide opportunities to achieve accurate localization. By combining the multiple readings of phase measurements, recent work cancels out the noise and achieve cm-level accuracy [42]. Instead of aiming at a higher localization accuracy, *TagBreathe* draws strength from those works and extends to breath monitoring.

Passive RFID tags feature low cost, light and small form factors which are ideal for non-intrusive breath monitoring. Once seamlessly attached on a user's cloth, a passive lightweight tag is hardly intrusive to the user. Fashion and textile industries start to embed RFID chips into fabrics for RFID clothing, which provides opportunities for non-intrusive cost-effective healthcare monitoring [8], [25].

Passive tags harvest energy from a commodity reader and backscatters incoming radio waves to send messages. The commodity reader measures the phase information of the backscattered signal at the physical layer and reports the phase value for each successfully identified tag. Suppose that the distance between the reader antenna and the tag is $d$. As radio waves traverse back and forth between the reader antenna and the tag in backscatter communication, the radio waves traverse a total distance of $2d$. Then the reader outputs a phase value of the backscatter radio wave as follows

$$\theta = \left(\frac{2\pi}{\lambda} \times 2d + c\right) \bmod 2\pi, \qquad (1)$$

where $\lambda$ is the wavelength, and $c$ is a constant phase offset which captures the influence of reader and tag circuits independent of the distance between the reader antenna and the tag. The phase value repeats with a period of $2\pi$ radians
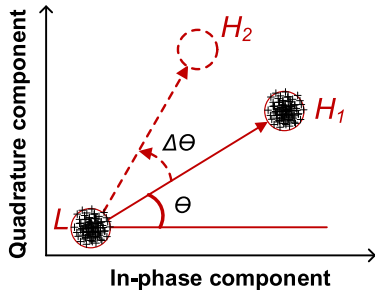
Fig. 1. Illustration of low level data measurements.



Fig. 2. Raw RSSI readings during the measurements.

every $\lambda/2$ in the distance of backscatter communication. COTS RFID readers (e.g., Impinj R420 [1]) can be programmed to output the low level data for application development. In the presence of multiple tags, readers avoid collisions with the standard RFID protocol and report phase values without interference. *TagBreathe* aims to leverage the COTS RFID systems to measure the phase values from RFID tags attached to users' clothes and simultaneously monitor breathing of multiple users.

## 3 SYSTEM OVERVIEW

The intuition of *TagBreathe* is that radio waves reflect off commodity tags attached to human body and thus the phases of the radio waves will be modulated by body movements of breathing. By carefully analyzing the data streams of phase values, we aim to extract the breathing signals with the following three key techniques, which we will elaborate in Section 4.

*1) Phase Measurement and Preprocessing.* COTS RFID readers measure the phase values of backscattered signals from the tags attached to users' clothes. COTS RFID readers report the phase value of each tag identification as well as the time stamp of the phase measurement. *TagBreathe* continuously reads the phase values and groups the phase values according to different users in the presence of multiple users. The changes in phase values indicate the body movements.

*2) Breath Signal Extraction. TagBreathe* extracts the breathing signals based on the observation that the phase values are influenced by the periodic changes introduced by the chest during inhaling and exhaling. We leverage our prior knowledge of human breathing rates and adopt a low pass filter to extract the breathing signals.

*3) Enhance Monitoring with Multiple Tags.* To mitigate the impact of packet loss and blockage of line-of-sight path in practice, *TagBreathe* attaches multiple tags to each user. We use multiple antennas to ensure a full coverage of the monitoring area. The antennas are scheduled by commodity readers and work in a round robin manner without antenna-to-antenna interference. *TagBreathe* combines the multiple data streams from the array of tags to enhance monitoring robustness in practical scenarios.

## 4 THE *TAGBREATHE* SYSTEM

### 4.1 Low Level Data Characterization

COTS RFID readers report low level information (e.g., received signal strength, phase value, Doppler shift, etc.) for each successfully identified tag to support various applications.
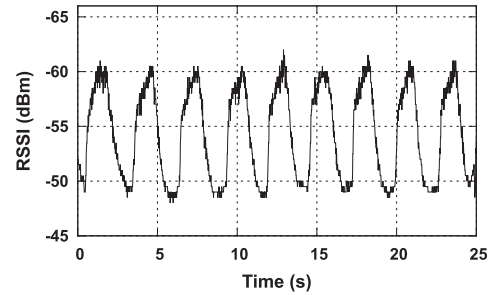
RFID tags modulate incoming radio signals by either reflecting or absorbing the radio signals which results in two possible states (i.e., *High* ($H$) and *Low* ($L$)) [19], [27]. The physical layer symbols (denoted by crosses in Fig. 1) exhibit two clusters (i.e., $H_1$ and $L$) in the constellation map as illustrated in the figure. The magnitude of vector $\overrightarrow{LH_1}$ measures the received signal strength, while $\theta$ measures the phase value of the backscatter signals. Due to Doppler frequency shift, one symbol cluster may rotate (e.g., from $H_1$ to $H_2$) in the constellation map during one packet transmission. As illustrated in the figure, $\Delta\theta$ measures the phase rotation which indicates the Doppler frequency shift in the constellation map [3].

In the initial experiment, a user attached with a passive tag on his cloth naturally breathes sitting 2m away from a reader's antenna. We collected the low level readings using the Impinj R420 reader for 25 seconds. The data sampling rate was around 64 Hz, i.e., 64 readings per second. The sampling rate is sufficiently high to capture the relatively low breathing rates of human subjects (e.g., around 10 - 20 breaths per minute). The low level data reports the received signal strength, raw phase value, raw Doppler shift, time stamp, and the tag ID.

*1) Received signal strength.* Fig. 2 plots the collected received signal strength indicator (RSSI) data which shows clear trend of periodic changes in the RSSI readings. That is because when the user inhales the body gets closer to the reader's antenna and thus the strength of backscatter signals increases, while the user exhales the RSSI readings decrease. The initial experiment shows that it is possible to track the breathing patterns with RSSI readings in the ideal scenario. The limit of RSSI measurement is its high sensitivity and low resolution. For instance, the resolution of the COTS reader is only 0.5 dBm. Due to the low resolution and sensitivity of RSSI readings, it is hard to precisely extract the subtle body movements in more challenging working scenarios.

Therefore, although the RSSI measurement results show clear trend of periodic changes (Fig. 2) in ideal experiment settings (e.g., 1m, line-of-sight paths), RSSI measurement suffers from high sensitivity and low resolution as the communication distance increases. It is hard to precisely extract the subtle body movements in more challenging working scenarios.

*2) Doppler frequency shift.* Fig. 3 plots the raw Doppler frequency shifts whose envelope roughly tracks periodic changes. COTS readers calculate the Doppler frequency shift with the phase rotation during one backscatter packet transmission as follows [1]
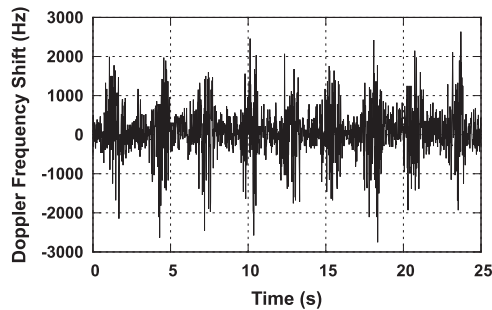
$$f = \frac{\Delta\theta}{4\pi\Delta T}, \tag{2}$$

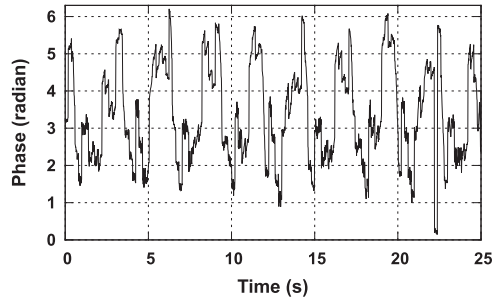Fig. 3. Raw Doppler frequency shift during the measurements.



Fig. 5. Channel hopping during the measurements.



Fig. 4. Raw phase values during the measurements.



Fig. 6. Displacement values during the measurements.

where $f$ denotes the Doppler frequency shift, $\Delta\theta$ denotes the phase rotation during one backscatter packet transmission, and $\Delta T$ denotes the duration of the packet transmission. In the figure, we see that although the raw Doppler frequency shifts are noisy, we can still observe some periodic changes in the measurement data. The limit of Doppler frequency shift measurement is that as the duration of a packet transmission $\Delta T$ is relatively small, the measured phase rotation $\Delta\theta$ during the one packet transmission is not reliable and may be subject to noises in practice. As such, the Doppler frequency shift requires relatively high moving speeds of RFID-labeled objects to generate notable $\Delta\theta$ during the short duration of packet transmissions. In more challenging scenarios, Doppler shift cannot provide reliable patterns of breathing.

*3) Phase values.* Fig. 4 plots the phase values during the measurement. Due to the channel frequency hopping, the phase values discontinuously changes when the reader hops to next channels, even when the tag is static. As specified in the standard EPC protocol [4], COTS readers hop among frequency channels to mitigate frequency selective fading and co-channel interference. Fig. 5 plots the channel indexes which show that the reader hops among 10 frequency channels and resides in each channel for around 0.2s. When the reader hops to neighbor channels, the wavelength $\lambda$ and the phase offset $c$ in Eq. (1) also change, leading to discontinuity of phase values every 0.2s [39]. A fixed frequency channel may not be supported by commodity readers in some regions (e.g., US, Singapore, Hong Kong) [4], since a continuous radio wave at a certain frequency may cause co-channel interference and violate radio frequency regulations.

To continuously track body movements without being interrupted by channel hopping, we first group the phase values according to channel indexes. Then, we calculate the displacement during two consecutive phase readings in the same channel according to Eq. (1). As the body movement speed is relatively low and the sampling rate is high (e.g., >
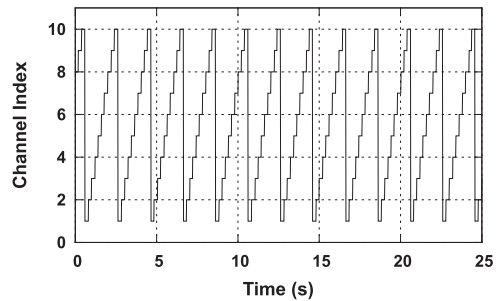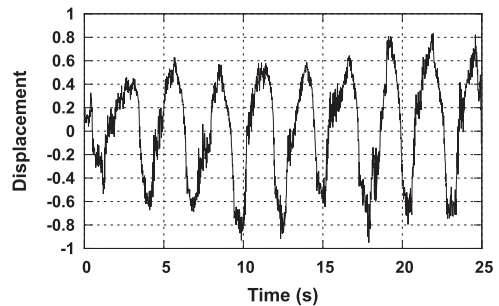
60 Hz), the tag displacement during two consecutive phase readings is within a half of radio wavelength. Thus, we calculate the displacement during two consecutive phase readings as follows

$$\Delta d_{i+1} = d_{i+1} - d_i = \frac{\lambda}{4\pi}(\theta_{i+1} - \theta_i), \qquad (3)$$

where $\Delta d_{i+1}$ denotes the displacement at time $i + 1$, and $\theta_{i+1}$ and $\theta_i$ denote the two consecutive phase readings measured in the same frequency channel. Then we measure the total displacement during $N$ readings as follows

$$D_j = \sum_{i=1}^{N} \Delta d_{i+j}. \qquad (4)$$

Note that in the standard EPC protocol, although the reader hops among different channels, within each channel, the phase offset remains the same in the two consecutive phase readings and we can calculate the corresponding displacement. When the phase reading hops to another channel, a gap is introduced when we calculate the displacement between the last phase reading of the current channel and the first phase reading of the next channel because of different phase offsets in the different channels. To address this problem, we note that the displacement is only calculated based on the phase values collected within the same channel with the same phase offset.

We normalize the displacement values and plot the results in Fig. 6. We see that the displacement values are not influenced by the frequency hopping and track the periodic body movement mainly due to breathing.

### 4.2 Breath Signal Extraction

We analyze the displacement values collected during the measurements with the Fourier transform (FFT). Fig. 7 shows
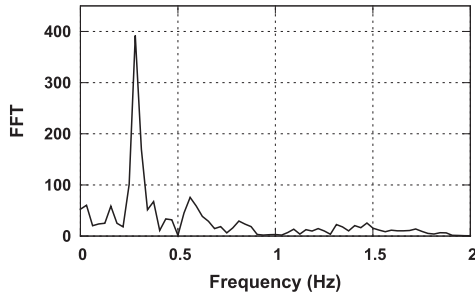
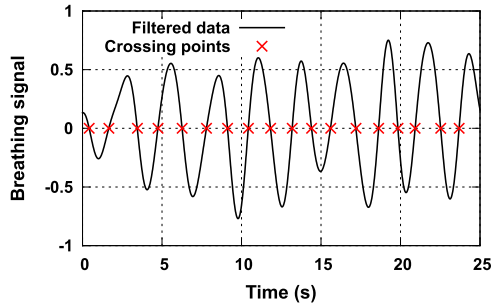Fig. 7. FFT for displacement values collected during the measurements.



Fig. 8. Extracted breathing signal from the measurements.

the FFT results. In the figure, the peak of the FFT output corresponds to the breathing rate. One of the pitfalls of the Fourier transform for a window size of $w$ seconds is that it has a resolution of $1/w$. In other words, a wider window provides better frequency resolution but poor time resolution. In our initial experiment, since the window size is 25 seconds, the frequency resolution is 0.04 Hz which corresponds to 2.4 breaths per minute. Such a low resolution means that if we measure breathing rates by identifying the peak in FFT (e.g., Fig. 7), the breathing rates will be grouped into FFT bins every 2.4 breaths per minute, which is not sufficient in practice. One straightforward way of improving the resolution is to increase the window size. Yet, increasing the window size causes longer delay, meaning that an apnea event can only be detected once every 25 seconds or more. Thus, it is challenging to balance the frequency resolution and time resolution by setting an appropriate window size.

Instead of measuring the breathing rate by finding the peak of FFT outputs, we apply an FFT-based low pass filter to filter out high frequency noises and then extract the breathing signals. We note that the typical breathing rate for a healthy person at rest is around 12 - 20 breaths per minute and generally lower than 40 breaths per minute. Thus, we first apply the FFT to convert the time domain displacement values to the frequency domain and set the cutoff frequency of the low pass filter as 0.67 Hz. After that, we use an inverse FFT (IFFT) to convert back to the time domain displacement values. Fig. 8 plots the extracted breathing signals after applying the low pass filter. In the figure, we see that noise is successfully filtered out. The extracted signal exhibits clear trends and we can apply time domain analysis to study the breathing signal. A finite impulse response (FIR) low pass filter can also be adopted to extract breathing signals.

To monitor breathing rates, we detect the zero crossings as plotted in Fig. 8. We record the time stamps of the zero
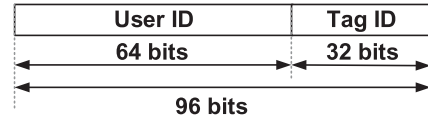


Fig. 9. *TagBreathe* overwrites 96-bit tag ID with 64-bit user ID and 32-bit short tag ID.

crossing events as $t_i$ and calculate the instant breathing rate as follows

$$\overline{f_{BR}}(t_i) = \frac{M - 1}{2(t_i - t_{i-M})}, \tag{5}$$

where $M$ denotes the number of buffered zero crossings. To enhance the robustness, we buffer 7 zero crossings which correspond to 3 breaths to calculate the breathing rates for realtime visualization.

### 4.3 Enhance Monitoring with Sensor Fusion of Multiple Tags

In the following, we describe how to enhance breath monitoring with sensor fusion of data streams from multiple RFID tags. Intuitively, instead of only using one tag for each user, we form an array of tags by attaching multiple RFID tags for each user to improve signal strengths and ensure that some tags can be read to mitigate the impact of blockage line-of-sight paths. To this end, we aggregate the data streams from the tags and fuse them so that the raw data streams reenforce each other and enhance the periodic signals due to body movements. By doing so, we improve the monitoring performance especially in the extraction of weak breathing signals.

The sensor fusion of multiple tags however can be very challenging, if the tags are randomly placed or their tag IDs are not organized as described in the paper. First, there might be multiple tags attached to multiple users in our targeted scenarios. Thus, it can be challenging to identify and group multiple tags attached to the same user and conduct sensor fusion accordingly, if the tags are not pre-loaded with the same user ID. Second, the displacement of multiple tags can add up destructively, if the tags are attached on arbitrary places on users. Third, the sensor fusion process may involve high computational cost if not handled efficiently. One may extract breathing signals from each data stream, and fuse the results in the final fusion phase. The breathing signal extraction involves relatively high computational overhead.

To address this problem, 64-bit user ID and 32-bit short tag ID are pre-loaded by overwriting the 96-bit tag ID. By doing so, the tags attached on the same user can be easily identified and grouped together which facilitates sensor fusion. We place the tags on the chest of the user so that the displacement of multiple tags can add up constructively. In the sensor fusion process, instead of extracting breathing signals for each tag and then combine the extracted signals, we propose to conduct the low level sensor fusion, and then extract breathing signal, which reduces the computation overhead otherwise involved in the multiple extraction processes.

In specific, we attach an array of tags consisting of $n$ RFID tags, $\{T_1, T_2, \ldots, T_n\}$ to a user. We overwrite the 96-bit tag ID with a 64-bit user ID followed by a 32-bit short tag ID as shown in Fig. 9. The 64-bit user ID allows us to differentiate
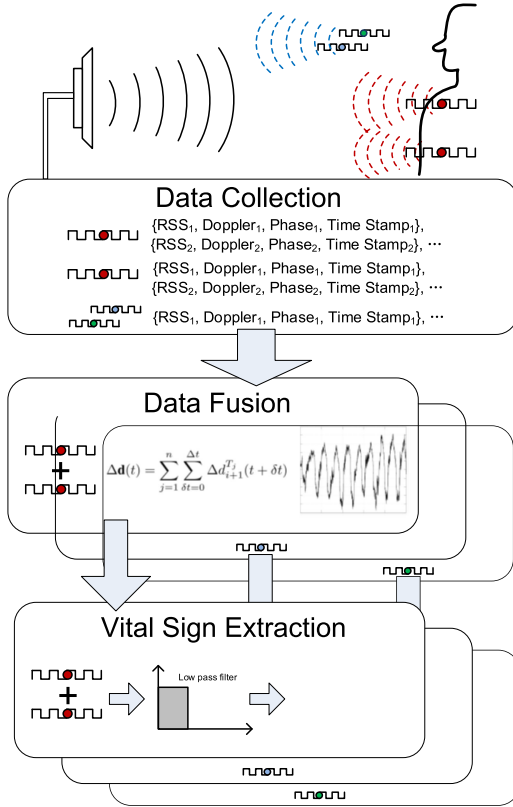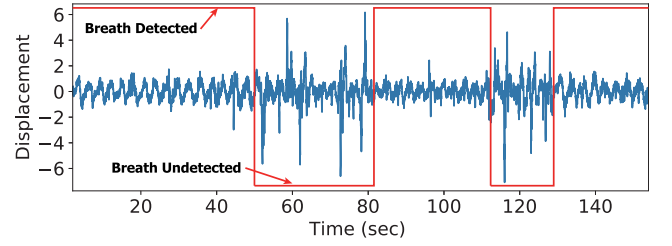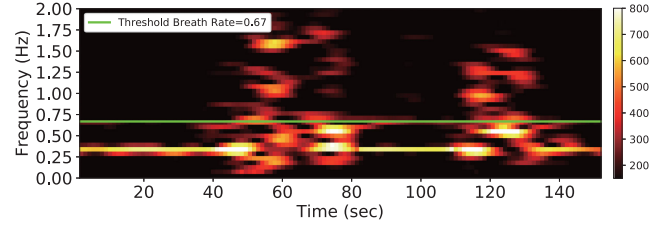
Fig. 10. Illustration of *TagBreathe* workflow.



(a) Displacement values and corresponding segmentation results.



(b) Spectrogram of the displacement

Fig. 11. Displacement values and corresponding spectrogram.

users and group the $n$ tags for each user. The 32-bit tag ID allows us to differentiate the tags and calculate the displacement values of each tag. By doing so, once a tag is identified, the low level data can be classified according to the user ID and the tag ID. We group the sensor data for the same user according to the 64-bit user ID and fuse $n$ data streams from $\{T_1, T_2, \ldots, T_n\}$ to enhance the monitoring performance. In the presence of multiple users, the low level data can be fused according to different users by examining user IDs. Thus, we focus on the sensor fusion of multiple tags for the same user. Note that overwriting tag IDs is a standard RFID operation supported by commodity RFID systems (e.g., Impinj R420). If the overwriting operation is not supported, the reader can build a mapping table to map and lookup 96-bit tag IDs to user IDs and short tag IDs.

In the process of data fusion, we first calculate the displacement values for each tag according to Eq. (3). The displacement value for tag $T_j$ collected during the time period $[t, t + \Delta t]$ is denoted as $\Delta d_{i+1}^{T_j}(t + \delta t), 1 \leq j \leq n, 0 \leq \delta t \leq \Delta t$, where $\Delta t$ is a certain time interval with short period. In practice, a normal person usually breathes 12~20 times per minute, resulting in 3~5 seconds per breath. In our experiment, we test multiple values of $\Delta t$ (i.e., 0.5s, 1s, 2s) and our system achieves the best performance when $\Delta t = 1$s. Therefore, the $\Delta t$ in our experiment is set to 1s. We aggregate the displacement values from $n$ tags for the time interval $[t, t + \Delta t]$ and fuse them together as follows

$$\Delta \mathbf{d}(t) = \sum_{j=1}^{n} \sum_{\delta t=0}^{\Delta t} \Delta d_{i+1}^{T_j}(t + \delta t). \tag{6}$$

Then we measure the total displacement during $N$ time intervals (i.e., $[t, t + N\Delta t]$) as follows

$$\Delta \mathbf{D}(t) = \sum_{i=0}^{N} \Delta \mathbf{d}(t + i\Delta t). \tag{7}$$

We process the fused data stream $\Delta \mathbf{D}(t)$ sampled at every $\Delta t$ and extract breathing signals using the breathing signal extraction algorithms (Section 4.2).

Fig. 10 illustrates the overall workflow. *TagBreathe* interrogates multiple RFID tags attached to users and collects low level data from those tags (Section 4.1). *TagBreathe* groups the readings according to user ID and carries out raw data fusion by synthesizing multiple data streams (Section 4.3). *TagBreathe* analyzes the synthesized data stream and extracts breathing signals for each user (Section 4.2).

### 4.4 Breathing Signal Segmentation

In a relatively static environment, only the chest movement introduced by the respiration of the monitored individuals dominates the source of motion, which can be captured by our TagBreath system [20]. However, such a tiny movement is hard to detect when a user is performing activities with relatively large body motion (e.g., walking), which dominates the received signal phase. In Fig. 11a, during a period of 160s, we ask a volunteer to sit 1m away in front of an RFID reader with 3 tags attached on his chest. The volunteer sits in a chair for a while and walks randomly for a few seconds within the communication area. As the blue line shown in Fig. 11a, we observe clear periodical pattern of the chest displacement when the volunteer is sitting in a chair, while it exhibits non-periodic pattern during walking.

Note that our system can reliably capture human respiration only when people are in static (e.g., sitting in the chair). In a dynamic environment (i.e., people are walking), *TagBreathe* cannot reliably detect human respiration due to large body movement. To address this problem, we need to determine whether a user is moving or remains static. If the user is in static (meaning that breathing signal can be segmented), the segmentation method detects such static events and

starts respiration monitoring; If the user is moving (meaning that breathing signal will be submerged due to large body movement), we temporarily stop respiration monitoring, and resume the monitoring when reliable results can be measured.

To detect whether a user is in static or dynamic, we exploit an efficient method called *Short-Time-Fourier-Transform* (STFT) to segment and identify chest displacement exactly derived from the static environment. STFT divides the signal into multiple segments with the same length and applies FFT on each segment such that the instantaneous frequency of the signal can be extracted. The key idea is that the frequencies of the chest displacement should mainly distribute in a narrow band if it is dominated by respiration while scattering over a relatively broader frequency band in dynamic environment (i.e., walking). This is because the RF signals reflected from the human chest result in diverse frequencies during walking activity. In STFT, we set the number of chest displacement points in each segment to 1024 (approximate 10 seconds) to achieve high resolution frequency. We choose the overlapping ratio of $15/16$ to increase the time resolution by $15\times$. When performing FFT on each segment, we use Hamming window to reduce the spectral leakage of the signal frequency. Fig. 11b shows the *spectrogram* of the chest displacement in Fig. 11a (the blue line). Each bin indicates the instantaneous intensity of a particular frequency at a particular time, where a brighter color represents a higher intensity in Fig. 11b.

In Fig. 11b, we observe that the frequencies primarily distributed around 0.25Hz (high intensity) during $0 \sim 40s$ and $80 \sim 110s$, indicating a clear periodic pattern of the chest displacement. On the other hand, the frequency distribution exhibits dispersive pattern during walking between $0 \sim 2$Hz. Therefore, we can effectively segment the respiration corresponded signal in static environment by using this unique pattern in the frequency domain. A normal person has less than 40 breaths per minute, hence, human respiration introduces frequency components of no more than $40/60 = 0.67$Hz, as the green line shown in Fig. 11b. If the total frequency intensity between 0 to 0.67Hz exceeds a threshold intensity, we regard the corresponding chest displacement as breathing signal and calculate the respiration rate in the time domain (described in Section 4.2). Otherwise, our *TagBreathe* system stops calculating the respiration rate. Note that we can roughly set an intensity threshold instead of a precise one. This is because a rough threshold have almost no impact on the segmentation result due to the prominent distinction of frequency intensity below 0.67Hz. With this method, the respiration corresponded signal is successfully segmented, as the red line shown in Fig. 11a.

### 4.5 Discussion

*1) Tag placement.* After many trials with different users, we find that some users breathe with chests while other breathe with their abdomens. To better capture the breathing patterns, we place three tags on the upper body of each user: one on chest, one on lower abdomen, and one in between. Note that when a user inhales or exhales, the three tags' relative displacement to reader's antenna simultaneously decrease and increase, which allows us to constructively fuse the sensor data and enhance the breathing signals.

*2) Enhancement with RSSI and Doppler frequency shift.* Tag-Breathe mainly uses the displacement values inferred from the phase values to monitor breathing. In the low level data characterization (Section 4.1), we notice that although RSSI and Doppler frequency shifts have their limits, they are also informative in the experiments. One possible enhancement is to fuse the RSSI and Doppler frequency shift with the phase values to improve the monitoring accuracy.

*3) Multiple antennas.* To increase communication coverage, a commodity reader can be connected to multiple antennas (e.g., 4 antenna ports for one Impinj R420 [1] reader). The reader coordinates the multiple antennas with the round-robin scheduling and avoids the inter-antenna interference. In other words, only one antenna will be powered up at a time and the power consumption of the RFID system will not increase with the number of antennas. Note that *TagBreathe* does not strictly require multiple antennas to monitor breathing. *TagBreathe* works well as long as the tags can be read successfully. The low level data is reported with the antenna port information. Thus, *TagBreathe* fuses the data according to the antenna port. As the antennas are distributed geographically, the data qualities of antennas vary across different users in different locations. *TagBreathe* evaluates the data quality in terms of received signal strength and data sampling rate and extract breathing signals with the data reported by the optimal antenna for each user.

*4) Multiple tags and readers.* Multiple tags and multiple readers can be used to increase the coverage region and enhance the sensing capability by creating more line-of-sight paths. Although multiple readers are promising to increase the coverage region and enhance the sensing capability by creating more line-of-sight paths, the cost of adding a new reader or extra antennas is much higher than adding multiple tags. In contrast, the cost of using multiple tags is very low and each tag costs only around 5 cents. Besides, placing multiple tags on the upper body of each user (i.e., one on chest, one on lower abdomen, and one in between) can better capture the breathing patterns. Note that when a user inhales or exhales, the tags' relative displacement to reader's antenna simultaneously decreases and increases, which allows us to constructively fuse the sensor data and enhance the breathing signals. However, the displacement of chest using multiple readers may be destructively cancelled due to certain locations of the readers and can make the sensor fusion complicated.

However, deploying multiple readers can increase the communication coverage, which can capture the breath patterns at different body orientation. On the contrary, using multiple tags may fail to capture the respiration patterns due to NLOS. As the LOS paths are mostly ensured in our experiments, we place multiple tags rather than multiple readers.

## 5 IMPLEMENTATION

We implement *TagBreathe* using COTS RFID systems.

*1) Hardware.* We use the Impinj Speedway R420 RFID reader [1] to interrogate commodity passive tags [2]. Fig. 12 depicts the prototype system. We evaluate different types of commodity passive tags (e.g., Alien 9640, Alien 9652, Impinj H47 tags). As the performance with different tags was comparable, we report the experiment results with the Alien 9640
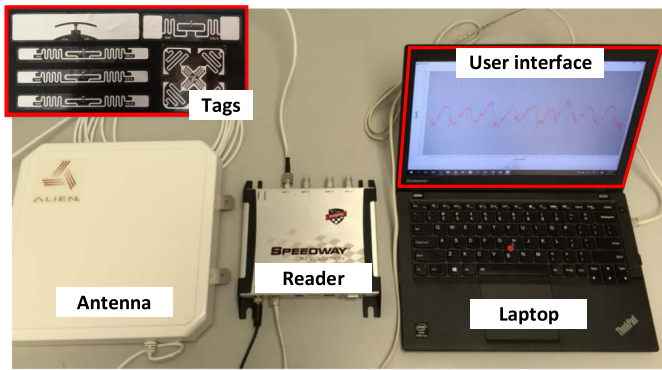
Fig. 12. *TagBreathe* prototype system.

TABLE 1
System Parameters and Default Experiment Settings

| Parameter | Range | Default |
|---|---|---|
| Channel | channel 1 - channel 10 | Hopping |
| Tx power | 15 - 30 dBm | 30 dBm |
| Distance | 1m - 6m | 4m |
| Orientation | 0° (front) - 180° (back) | front |
| Number of users | 1 - 4 users | 1 user |
| Tags per user | 1 - 3 tags | 3 tags |
| Breathing rate | 5 - 20 bpm | 10 bpm |
| Posture | Sitting, Standing, Lying | Sitting |
| Propagation path | with/without LOS path | with LOS path |

passive tags. The RFID system operates at the Ultra-High Frequency (UHF) band between 902 MHz and 928 MHz [1]. Both the reader and the tags follow the standard EPC protocol, which arbitrates tag-to-tag collisions at the MAC layer. We config the transmission power to 30 dBm. The reader supports upto 4 directional antennas. In our prototype implementation, we adopt the Alien ALR-8696-C circular polarized antenna with the antenna gain of 8.5 dBic. As the communication range is around 10m, the reader can cover a relatively large area with multiple antennas. The reader sends the low level data with time stamps to the laptop (Leveno X240) via Ethernet cable. *TagBreathe* processes the low level data and extracts breathing signals in realtime.

*2) Software.* We implement *TagBreathe* based on the LLRP Toolkit (LTK) [3], [42] to config the commodity reader and read the low level data. The LTK communicates with the reader following the LLRP protocol [2]. We program the reader to continuously identify tags in the communication range and report the low level data (e.g., received signal strength, phase value, Doppler shift, etc). The low level data are processed with the *TagBreathe* algorithms implemented in Java. We implement all the components (e.g., preprocessing, sensor fusion, breath signal extraction, etc.) which execute in a pipelined manner. The results are computed and visualized as shown in Fig. 12, which shows extracted breathing signals in realtime.

## 6 EVALUATION

### 6.1 Experiment Setting

To evaluate the performance of *TagBreathe*, we recruit 4 volunteers. The volunteers wear their daily clothes (e.g., T-shirts, jackets, baggy cloths) in various fabric materials.

Various numbers of COTS tags are attached to different parts on their cloths during the experiments. To evaluate the accuracy of *TagBreathe*, we use a breathing metronome application [10] to instruct the participants to regulate their breaths to evaluate the accuracy of breathing rate estimate of *TagBreathe*. We carry out the experiments in a standard office building. The office environment contains furniture including desks and chairs, and electric appliances including laptops and fans. We experiment with varied communication distances and different postures. The users naturally breathe following the instructions of the metronome application. Table 1 summarizes key system parameters and default experiment settings.

### 6.2 Experiment Results

The measurement accuracy is one of the most important metrics for the breathing rate monitoring. We calculate the accuracy as follows

$$Accuracy = 1 - \frac{|\hat{R} - R|}{R}, \qquad (8)$$

where $\hat{R}$ is our measurement result and $R$ is the actual breathing rate, respectively.

*1) Impact of low level data.* In the preliminary study of our work, we collect all low-level data of RF signal including signal phase, RSSI and Doppler frequency shift. The RSSI and Doppler frequency shift measurement show clear trend of periodic changes in ideal experiment. In this evaluation, we also collected all low-level data but in a relatively challenging practical scenarios. In this case, we attach three tags on a user's chest to capture breathing signals and the low-level data from $2m$ away with LOS paths. The RSSI, Doppler shift and phase of the RF signal are plotted in Fig. 13.



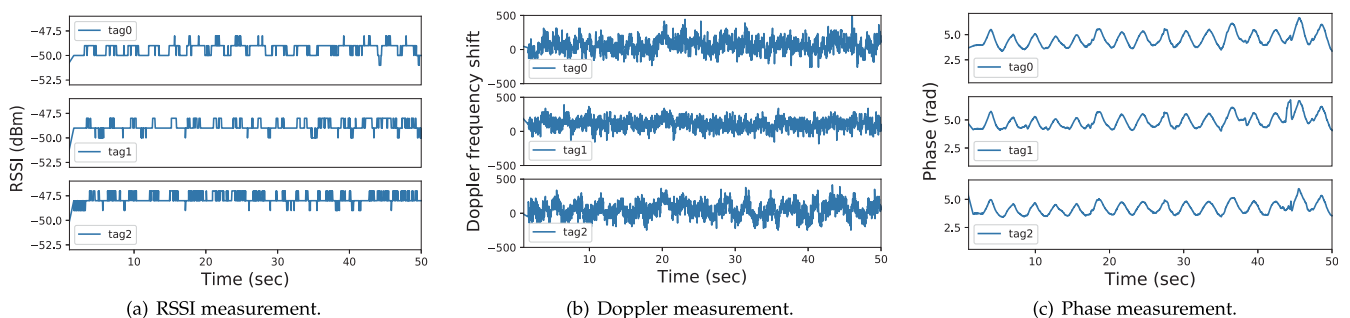| (a) RSSI measurement. | (b) Doppler measurement. | (c) Phase measurement. |

Fig. 13. Impact of different low level data.
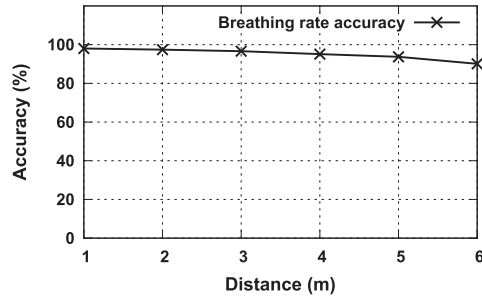
Fig. 14. Breathing rate accuracy at different distances.



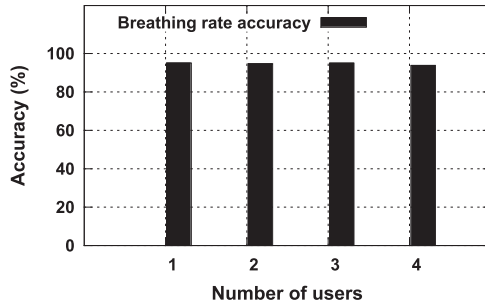Fig. 16. Breathing rate accuracy with different number of contending tags.



Fig. 15. Breathing rate accuracy with different number of users.

In Fig. 13a, the RSSI measurement shows no periodic pattern compared to the phase measurement in Fig. 13c. As the communication distance increases to $2m$, RSSI measurements suffer from low resolution, which makes it hard to extract the subtle body movements in more challenging scenarios. Similarly, Doppler shift cannot provide reliable patterns of breathing as shown in Fig. 13b. The Doppler frequency shift requires relatively high moving speeds of RFID-labeled objects, while the chest movement caused by human respiration is relatively slow. In contrast, the phase measurement in Fig. 13c exhibits more reliable periodic pattern, which is more suitable to capture tiny movement of human chest during respiration.

*2) Impact of distance.* We first evaluate the accuracy of breath monitoring at different distances from the reader's antenna to the tags attached to users. In the experiment, we fix the location of the antenna 1m above the ground and ask users to sit at different locations with the distances ranging from 1m to 6m away from the antenna. In each experiment, the user breathes according to a metronome mobile application running on a smartphone. The breathing rates range from 5 to 20 breaths per minute (bpm). Each experiment lasts for two minutes. We continuously measure the breathing signals and compute the average breathing rates using *TagBreathe*. We repeat the experiments for 100 times. During the experiments, we collect around 500,000 low level readings in total.

We compare the experiment results of *TagBreathe* with the ground truth and plot the accuracies at different distances in Fig. 14. According to the experiment results, the accuracy of breathing rate measurement is 98.0 percent at 1m. Although the accuracy decreases slightly as the distance increases, the experiment results show that the accuracy remains higher than 90.0 percent throughout the experiments. As the communication range increases, the reader observes weaker backscatter signal strengths and lower reading rates of low
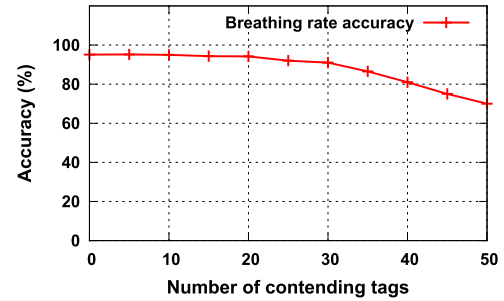
level data, which negatively affects the breathing signal extraction.

*3) Impact of the number of users.* We evaluate the performance of *TagBreathe* with multiple users. The users sit side by side 4m away from the antenna. Each user wears three commodity passive tags. A commodity reader reads the low level data from all the tags and groups the data according to the user IDs extracted from the tag IDs. We evaluate the monitoring accuracies with different number of users in Fig. 15. According to the experiment results, the breathing rate accuracies with different number of users remain around 95.0 percent. Thanks to the RFID collision avoidance protocol, the backscattered signals from different users do not interfere with each other. Moreover, the experiment results indicate that the reading rate of commodity reader is sufficiently high to simultaneously monitor breathing even with 4 users wearing 12 tags.

Compared with previous wireless sensing techniques, our system can simultaneously monitor respiration rates of multiple users. Our system performs well because it is compatible with the EPC protocol and benefit from the collision arbitration to avoid interferences among multiple tags. In addition, by attaching multiple tags for each user, our system can create more line-of-sight paths and enhance the sensing capability by sensor fusion.

*4) Impact of contending tags.* To evaluate the impact of lower reading rates due to an increasing number of tags in presence, we label daily items with RFID tags and place the RFID-labeled items in the communication range of the commodity reader. Same as the breath monitoring tags attached to users, the item-labeling tags in the communication range contend for wireless channels following the standard EPC protocol. As a result, the reading rates decrease as the number of contending tags increases in the communication range. In the experiments, a user wears 3 tags and sits in front of the antenna. We vary the number of RFID tags and repeat the experiments with different number tags. The commodity reader continuously monitors all the tags and reads low level data from them including the ones used for labeling the daily items. Before the experiments, we overwrite the tag IDs of the 3 breath monitoring tags so that the reader can identify them and monitor breathing rates. Fig. 16 plots the measurement accuracy with different number of contending RFID tags in presence. According to the experiment results, we find that *TagBreathe* is able to achieve the accuracy of 91.0 percent even with 30 contending tags in the communication range. The main reason is because the total reading rates is sufficiently high and *TagBreathe* can collect sufficient readings from the
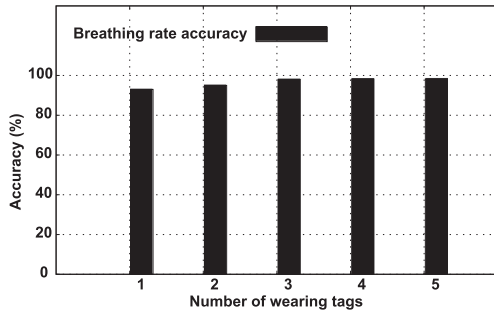
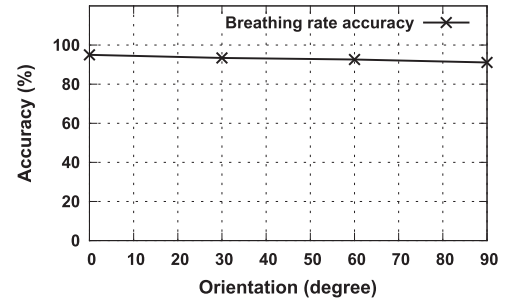Fig. 17. Breathing rate accuracy with different number of wearing tags.



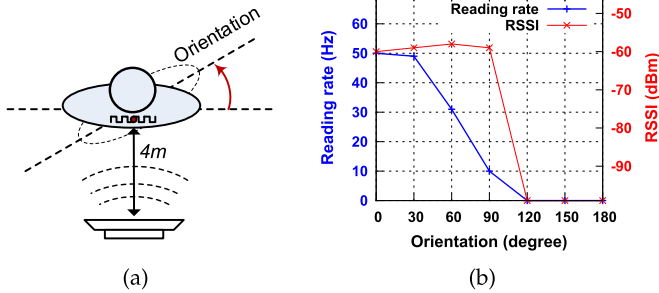Fig. 19. Accuracy at different orientation.



Fig. 18. Reading rate and RSSI at different orientation.

breath monitoring tags. The accuracy decreases when more contending tags are in presence which leads to lower reading rates of 3 breath monitoring tags.

In addition, we evaluate the impact of number of wearing tags. In our experiment, we ask the volunteer to sit 1m away from the reader. We vary the number of tags attached on the user's chest from 1 to 5 and repeat the experiment for each number of tags. Fig. 17 shows the experiment result. We observe that, with the number of wearing tags increases, the measured accuracy increases accordingly. This is because the aggregated displacement from multiple tags can provide more reliable patterns of human respiration than a single tag. When the number of tags exceeds 3, we observe that the accuracy is sufficiently high. Therefore, in our evaluation, we attach 3 tags on the user's chest.

*5) Impact of tag orientation and line-of-sight path.* The performance of RFID systems is influenced by antenna orientation as well as blockage of line-of-sight paths by human body. We evaluate the monitoring accuracy at different antenna orientation. For the evaluation purposes, we only connect one directional antenna to the reader to intentionally limit the coverage of the RFID system. In practical usage scenarios, we note that multiple antennas can be connected to fully cover the monitoring area. As illustrated in Fig. 18a, a user is 4m away from the antenna and repeats the experiments at different orientation. The user first faces to the antenna (i.e., 0°) and rotates counter-clockwise until the user faces the opposite direction (i.e., 180°). In Fig. 18b, we measure the reading rate of low level data as well as the RSSI of backscatter signals at different orientation. We observe as long as there are line-of-sight paths between the tags and the antenna (i.e., [0°, 90°]) the RSSI of the backscatter signal does not change much. On the other hand, the reading rate decreases from 50 Hz when the user faces to the antenna to 10 Hz when the user rotates to 90°. When the user further

rotates (e.g., [120°, 180°]), as the line-of-sight path path is blocked by the user's body, the reader cannot identify the tag or read low level data any more. In such cases (> 90°), *Tag-Breathe* does not report breath monitoring results.

Note that our current design cannot mitigate shadowing effects since the LOS path between the reader and tags might be obstructed by other users. The shadowing effects might be mitigated by deploying more readers with multiple antennas in the environment to increase the coverage and ensure LOS paths to the tags in practice. Besides, tag selection techniques can be applied to select the most relevant tags that are affected by human respiration and are not greatly impacted by the shadowing effects.

In practical usage scenarios, to increase the reader coverage and fully enable breath monitoring in the environment, a commodity reader can connect multiple antennas to ensure line-of-sight paths to the tags in practice. Note that the reader can coordinate the multiple antennas with the round-robin scheduling and avoid the inter-antenna interference. Moreover, as only one antenna will be powered up at a time and the overall power consumption of the RFID system will not increase with the number of antennas.

Fig. 19 plots the measurement accuracy with different tag orientation with line-of-sight paths (i.e., < 90°). According to the experiment results, when the user faces to the antenna, the measurement accuracy is above 90 percent. The accuracy decreases from 90 to 85 percent as the user rotates to 90°.

*6) Impact of combined parameters.* The combination of different parameters may cause different impacts on *TagBreathe* system. In this evaluation, we consider the effects of combining the communication distances and body orientations and have the following observations:

1) When the body orientation to the antenna is larger than 90°, the system performance dramatically degrades since the LOS paths are blocked by the human body. In this case, the tags cannot be read by the reader due to the blockage of line-of-sight paths, regardless of communication distance. Meaning that once the tags are blocked, the communication distance becomes irrelevant.

2) Similarly, when the communication distance is larger than 6m, the system performance is irrelevant to the body orientations since the received backscattered signal becomes very weak and sometimes the weak signals cannot be detected.

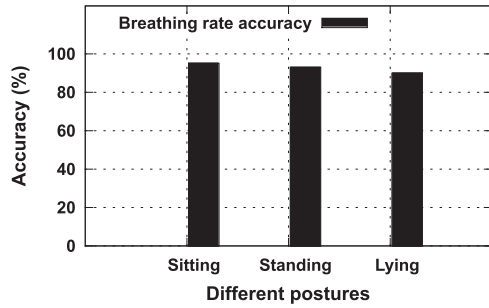3) When the communication distance is less than 6m and the body orientation is less than 90 degree,

Fig. 20. Accuracy at different postures.



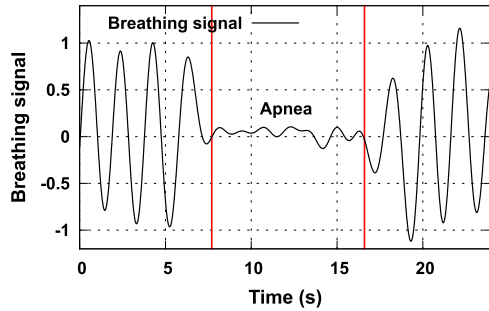Fig. 22. Apnea detection with different users.



Fig. 21. Apnea detection: The user first breathes normally, and holds breath for a while (6s - 16s). The signal magnitude drops dramatically during the period and the apnea event can be detected with a threshold detection method.

we observe the consistent impacts on the system performance. The system performance degrades as the communication distance increases under any certain body orientation less than 90°. Similarly, the system performance decreases with the body orientation increases under any certain communication distances less than 6m.

Therefore, in our evaluation, we only exhibit the most notable results by changing one parameter each time while keeping other parameters unchanged to observe how each parameter affects the system.

*7) Impact of different postures.* We evaluate the monitoring accuracy with different postures, i.e., sitting, standing, and lying. The location of the antenna is fixed around 1m above the ground and the communication range between the tags and the reader remains unchanged throughout the experiments. As such, the results are mainly influenced by the orientation of the tags to the antenna, as well as the breathing behaviors with different postures. According to the experiment results, the monitoring accuracy remains above 90.0 percent across different postures.

## 6.3 Case Study: Apnea Detection

We carry out a case study to detect the apnea event, which means the absence of breathing for at least 10 seconds [10]. We first extract the breathing signals with *TagBreathe* and track the magnitude of breathing signals. We detect the apnea events with the threshold based detection. In the experiment, a user wears 3 tags and sits $4m$ away from the antenna. We first run a training phase where *TagBreathe* collects $n$ breathing signal samples for 10 seconds (denoted as $\Delta\mathbf{D}[1,\ldots,n]$), and measures the magnitude of the breathing signal every 10-second window as $BSS = \max(\Delta\mathbf{D}[1,\ldots,n]) - \min(\Delta\mathbf{D}[1,\ldots,n])$.
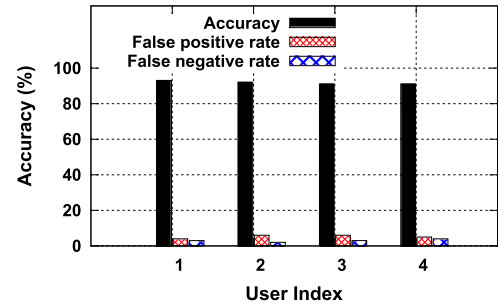
We detect an apnea event, if the magnitude of breathing signal drops by $\beta$ percent; if the magnitude of breathing signal remains stable, we say the user breathes normally. Note that the training phase involves only one-time cost to bootstrap the apnea detection. After that, we can continuously monitor the magnitude and update the threshold in practice.

To investigate the performance in detecting apnea events, the user first breathes normally, holds breath for around 10 seconds to simulate an apnea event, and resumes normal breathing. Fig. 21 plots the extracted breathing signals, where the user holds breath for around 10 seconds starting from 6s to 16s. We see the magnitude of breathing signal decreases substantially the period from 6s to 16s, which allows us to detect the apnea event using the threshold based detection method.

To measure the performance of apnea detection, we ask 4 users with different body types and breathing patterns to either breathe naturally or simulate apnea events by holding breaths for 10 seconds. Each experiment lasts for around 30 seconds. We evaluate accuracy, false positive rate, and false negative rate of the apnea detection. Fig. 22 plots the apnea detection results for the 4 users respectively. The experiment results show that *TagBreathe* achieves detection accuracy of 91.0 percent across different users. Both the false positive rates and the false negative rates are below 6.0 percent. After examining the collected data traces, we find that the false positive is mainly caused when the tags are blocked by human body due to some certain posture, the apnea detection method may trigger false alarms, since in this case no breathing signals can be measured and the detection method incorrectly considers such cases as apnea events. In this case, *TagBreathe* cannot always extract and track breathing signals. The false negative is incurred by the noise and interference (e.g., people walking nearby, environmental noises), which cause the fluctuation of the signal phase value, even when the apnea really happens. In this case, our system incorrectly detects these fluctuations as breathing. In order to accurately detect the apnea events, we need to ensure clear line-of-sight paths by deploying multiple antennas and adequate reading rates in practice.

## 7 RELATED WORK

Our work is mostly related to the recent development of RFID sensing applications based on RFID systems [11], [12], [16], [21], [22], [28], [30], [34], [35], [38], [42], [44], [46]. Tagoram [42] leverages COTS RFID systems to accurately

pinpoint RFID-labeled items, which supports automatic luggage handling and enables innovative human computer interactions. Tagball [21] labels physical objects with passive RFID tags and tracks the orientation and attitude of the objects to enable 3D human computer interaction. Tagyro [39] overcomes practical challenges such as imperfect radiation pattern of practical tags and enables orientation tracking in 3D space. R# [14] estimates the number of humans in various locations by examining backscattered radio waves. Tadar [43] tracks users' movement by building antenna arrays with RFID tags and analyzing their reflected radio signals. OTrack [30] tracks ordering of luggage with received signal strength of RFID tags. STPP [31] analyzes phase profiles with a mobile reader and calculates spatial ordering to determine the relative location of tags. MobiTagBot [32] carefully handles the multipath reflections and leverages frequency hopping to achieve accurate sorting of tags with a mobile reader. Those works build on COTS RFID systems and deliver the benefit of wireless sensing to users in a cost effective manner. Similar to those works, *TagBreathe* explores the possibility of breath monitoring for multiple users with COTS RFID systems.

Recent works monitor breathing rates by measuring wireless signals reflected from human body using Doppler radars or ultra-wideband radars [9], [13], [17], [45]. Those works typically transmit wireless signals to a user and capture miniature changes in reflected radio waves due to chest motion during breathing. To detect the small movements, such systems need high sampling rates which incur high power consumption. Vital-Radio [9] builds active radios to transmit frequency modulated carrier waves and detect small shifts in reflected frequency due to body movements. Those systems however require customized high-end active radios which are not readily available on the market and incur prohibitive cost. Those system cannot effectively differentiate whether the reflected signals are indeed from the subject under monitoring or due to the movements of other objects in the environment. As a result, those systems suffer low detection accuracy since movements in the environment would reflect radio waves and affect detection results. Recent works [9], [10], [23], [29], [33] leverage WiFi signals (e.g., received signal strength, channel state information) to estimate breathing rates. Although some works in the WiFi band, they need to transmit frequency modulated carrier waves [9] or use high-end software defined radios. Moreover, the WiFi-based monitoring approaches suffer low accuracy in the presence of multiple users. Recent works also explore the possibility of leveraging speakers and microphones available on smartphones to monitor respiration. C-FMCW (Correlation based Frequency Modulated Continuous Wave) method [36] measures the chest movement by sending acoustic chirps and detecting the reflection of chirps.

## 8 CONCLUSION

In this paper, we ask the question whether we can use COTS systems to wirelessly monitor breathing. We provide an affirmative answer by designing and implementing *TagBreathe*, which wirelessly senses breaths of multiple users with COTS RFID systems. *TagBreathe* follows the standard collision arbitration protocol and naturally separates the backscattered signals from lightweight passive tags, which allows us to simultaneously monitor breathing for multiple users. We carefully design signal processing algorithms to extract breathing signals from the low level data reported by commodity readers. *TagBreathe* further enhances monitoring performance with extensive sensor fusion of low level data streams. We have implemented and evaluated *TagBreathe* under various working scenarios. The experiment results demonstrate that *TagBreathe* can monitor breathing for multiple users and directly deliver the benefits of wireless sensing with COTS RFID systems.

## REFERENCES

[1]  Impinj. 2019. [Online]. Available: http://www.impinj.com
[2]  Alien Technology. 2019. [Online]. Available: http://www.alientechnology.com
[3]  LLRP Toolkit. 2019. [Online]. Available: http://www.llrp.org
[4]  EPCgloable C1G2 Standard. 2019. [Online]. Available: http://www.gs1.org
[5]  Cleveland Clinic. 2019. [Online]. Available: http://my.clevelandclinic.org
[6]  Breathe Deep to Lower Blood Pressure. 2019. [Online]. Available: http://www.nbcnews.com/id/14122841
[7]  Your Newborn Baby's Breathing Noises. 2019. [Online]. Available: http://www.webmdcom/parenting/baby/your-newborn-babys-breathing-noises
[8]  Researchers Unveil Breakthrough in Weaving NFC Chips into Cloths. 2019. [Online]. Available: http://www.nfcworld.com
[9]  F. Adib, H. Mao, Z. Kabelac, D. Katabi, and R. Miller, "Smart homes that monitoring breathing and heart rate," in *Proc. 33rd Annu. ACM Conf. Human Factors Comput. Syst.*, 2015, pp. 837–846.
[10]  H. Abdelnasser, K. Harras, M. Youssef, "UbiBreathe: A ubiquitous non-invasive WiFi-based breathing estimator," in *Proc. 16th ACM Int. Symp. Mobile Ad Hoc Netw. Comput.*, 2015, pp. 277–286.
[11]  K. Bu, B. Xiao, Q. Xiao, and S. Chen, "Efficient misplaced-tag pinpointing in large RFID systems," *IEEE Trans. Parallel Distrib. Syst.*, vol. 23, no. 11, pp. 2094–2106, Nov. 2012.
[12]  S. Chen, M. Zhang, and B. Xiao, "Efficient information collection protocols for sensor-augmented RFID networks," in *Proc. IEEE INFOCOM*, 2011, pp. 3101–3109.
[13]  A. Droitcour, O. Boric-Lubecke , G. Kovacs, "Signal-to-noise ratio in doppler radar system for heart and respiratory rate measurements," *IEEE Trans. Microw. Theory Techn.*, vol. 57, no. 10, pp. 2498–2507, Oct. 2009.
[14]  H. Ding, J. Han, A. X. Liu, J. Zhao, P. Yang, W. Xi, and Z. Jiang, "Human object estimation via backscattered radio frequency signal," in *Proc. IEEE Conf. Comput. Commun.*, 2015, pp. 1652–1660.
[15]  H. Ding, L. Shangguan, Z. Yang, J. Han, Z. Zhou, P. Yang, W. Xi, and J. Zhao, "FEMO: A platform for free-weight exercise monitoring with RFIDs," in *Proc. 13th ACM Conf. Embedded Netw. Sensor Syst.*, 2015, pp. 141–154.
[16]  C. Duan, L. Yang, and Y. Liu, "Accurate spatial calibration of RFID antennas via spinning tags," in *Proc. IEEE 36th Int. Conf. Distrib. Comput. Syst.*, 2016, pp. 519–528.
[17]  R. Fletcher and J. Han, "Low-cost differential front-end for doppler radar vital sign monitoring," in *Proc. IEEE MTT-S Int. Microwave Symp. Digest*, 2009, pp. 1325–1328.
[18]  T. Gu, L. Wang, H. Chen, X. Tao and J. Lu, "Recognizing multi-user activities using Wireless body sensor networks," *IEEE Trans. Mobile Comput.*, vol. 10, no. 11, pp. 1618–1631, Nov. 2011.
[19]  Y. Hou, J. Ou, Y. Zheng, and M. Li, "PLACE: Physical layer cardinality estimation for large-scale RFID systems," in *Proc. IEEE Conf. Comput. Commun.*, 2015, pp. 1957–1965.
[20]  Y. Hou, Y. Wang, and Y. Zheng, "TagBreathe: Monitor breathing with commodity RFID systems," in *Proc. IEEE 37th Int. Conf. Distrib. Comput. Syst.*, 2017, pp. 404–413.

[21] Q. Lin, L. Yang, Y. Sun, T. Liu, X.-Y. Li, and Y. Liu, "Beyond one-dollar mouse: A battery-free device for 3D human-computer interaction via RFID tags," in *Proc. IEEE Conf. Comput. Commun.*, 2015, pp. 1661–1669.

[22] X. Liu, K. Li, H. Qi, B. Xiao, and X. Xie, "Fast counting the key tags in anonymous RFID systems," in *Proc. IEEE 22nd Int. Conf. Netw. Protocols*, 2014, pp. 59–70.

[23] X. Liu, J. Cao, S. Tang, J. Wen, and P. Guo, "Contactless respiration monitoring via off-the-shelf WiFi devices," *IEEE Trans. Mobile Comput.*, vol. 15, no. 10, pp. 2466–2479, Oct. 2016.

[24] M. L. R. Mogue, B. Rantala, "Capnometers," *J. Clinical Monitoring*, vol. 4, pp. 115–121, 1988.

[25] R. Nayak, A. Singh, R. Padhye, and L. Wang, "RFID in textile and clothing manufacturing: Technology and challenges," *Fashion Textiles*, vol. 2, no. 1, 2015, Art. no. 9.

[26] L. Ni, Y. Liu, Y. Lau, and A. Patil, "LANDMARC: Indoor location sensing using active RFID," *Wireless Netw.*, vol. 10, no. 6, pp. 701–710, 2004.

[27] J. Ou, M. Li, and Y. Zheng, "Come and be served: Parallel decoding for COTS RFID tags," in *Proc. 21st Annu. Int. Conf. Mobile Comput. Netw.*, 2015, pp. 500–511.

[28] S. Qi, Y. Zheng, M. Li, L. Lu, Y. Liu, "COLLECTOR: A secure RFID-enabled batch recall protocol," in *Proc. IEEE Conf. Comput. Commun.*, 2014, pp. 1510–1518.

[29] R. Ravichandran, E. Saba, K. Chen, M. Goel, S. Gupta, S. Patel, "WiBreathe: Estimating respiration rate using Wireless signals in natural settings in the home," in *Proc. IEEE Int. Conf. Pervasive Comput. Commun.*, 2015, pp. 131–139.

[30] L. Shangguan, Z. Li, Z. Yang, M. Li, and Y. Liu, "OTrack: Order tracking for luggage in mobile RFID systems," in *Proc. IEEE INFOCOM*, 2013, pp. 3066–3074.

[31] L. Shangguan, Z. Yang, A. X. Liu, Z. Zhou, and Y. Liu, "Relative localization of RFID tags using spatial-temporal phase profiling," in *Proc. 12th USENIX Conf. Netw. Syst. Des. Implementation*, 2015, pp. 251–263.

[32] L. Shangguan and K. Jamieson, "The design and implementation of a mobile RFID tag sorting robot," in *Proc. 14th Annu. Int. Conf. Mobile Syst. Appl. Services*, 2016, pp. 31–42.

[33] H. Wang, D. Zhang, J. Ma, Y. Wang, Y. Wang, D. Wu, T. Gu, and B. Xie, "Human respiration detection with commodity Wi-Fi devices: Do user location and body orientation matter?" in *Proc. ACM Int. Joint Conf. Pervasive Ubiquitous Comput.*, 2016, pp. 25–36.

[34] J. Wang, F. Adib, R. Knepper, D. Katabi, and D. Rus, "RF-compass: Robot object manipulation using RFIDs," in *Proc. 19th Annu. Int. Conf. Mobile Comput. Netw.*, 2013, pp. 3–14.

[35] J. Wang, D. Vasisht, and D. Katabi, "RF-IDraw: Virtual touch screen in the air using RF sensing," in *Proc. ACM Conf. SIGCOMM*, 2014, pp. 235–24.

[36] T. Wang, D. Zhang, Y. Zheng, T. Gu, X. Zhou, and B. Dorizzi, "C-FMCW based contactless respiration detection using acoustic signal," *Proc. ACM Interact. Mobile Wearable Ubiquitous Technol.*, vol. 1, no. 4, pp. 170:1–170:20, 2017.

[37] W. Wang, A. X. Liu, M. Shahzad, K. Ling, and S. Lu, "Understanding and modeling of Wi-Fi signal based human activity recognition," in *Proc. 21st Annu. Int. Conf. Mobile Comput. Netw.*, 2015, pp. 65–76.

[38] Y. Wang, Y. Zheng, "Modeling RFID signal reflection for contact-free activity recognition," *Proc. ACM Interactive Mobile Wearable Ubiquitous Technol.*, vol. 2, 2019, Art. no. 193.

[39] T. Wei and X. Zhang, "Gyro in the Air: Tracking 3D orientation of batteryless internet-of-things," in *Proc. 22nd Annu. Int. Conf. Mobile Comput. Netw.*, 2016, pp. 55–68.

[40] C. Wu, Z. Yang and C. Xiao, "Automatic radio map adaptation for indoor localization using smartphones," *IEEE Trans. Mobile Comput.*, vol. 17, no. 3, pp. 517–528, Mar. 2018.

[41] J. Yang, S. Sidhom, G. Chandrasekaran, T. Vu, H. Liu, N. Cecan, Y. Chen, M. Gruteser and R. P. Martin, "Detecting driver phone use leveraging car speakers," in *Proc. 17th Annu. Int. Conf. Mobile Comput. Netw.*, 2011, pp. 97–108.

[42] L. Yang, Y. Chen, X.-Y. Li, C. Xiao, M. Li, and Y. Liu, "Tagoram: Real-time tracking of mobile RFID tags to high precision using COTS devices," in *Proc. 20th Annu. Int. Conf. Mobile Comput. Netw.*, 2014, pp. 237–248.

[43] L. Yang, Q. Lin, X. Li, T. Liu, and Y. Liu, "See through walls with COTS RFID system!," in *Proc. 21st Annu. Int. Conf. Mobile Comput. Netw.*, 2015, pp. 487–499.

[44] L. Yao, Q. Sheng, W. Ruan, T. Gu, X. Li, N. Falkner, and Z. Yang, "RF-Care: Device-free posture recognition for elderly people using a passive RFID tag array," in *Proc. 12th EAI Int. Conf. Mobile Ubiquitous Syst.: Comput. Netw. Services*, 2015, pp. 120–129.

[45] M. Zhao, F. Adib, and D. Katabi, "Emotion recognition using Wireless signals," in *Proc. 22nd Annu. Int. Conf. Mobile Comput. Netw.*, 2016, pp. 95–108.

[46] Y. Zheng and M. Li, "Read bulk data from computational RFIDs," in *Proc. IEEE Conf. Comput. Commun.*, 2014, pp. 495–503.

**Yanwen Wang** received the BS degree in electronic engineering from Hunan University, Changsha, China, in 2010, and the MS degree in electrical engineering from the Missouri University of Science and Technology, MO, in 2013. He is currently working toward the PhD degree with the Department of Computing, Hong Kong Polytechnic University. His research interest includes mobile and network computing and RFID systems.
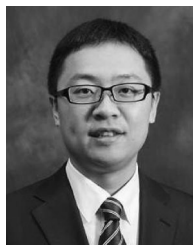
**Yuanqing Zheng** received the BS degree in electrical engineering and the ME degree in communication and information system from Beijing Normal University, Beijing, China, in 2007 and 2010, respectively, and the PhD degree from the School of Computer Engineering from Nanyang Technological University, in 2014. He is currently an assistant professor with the Department of Computing, Hong Kong Polytechnic University. His research interest includes mobile and network computing, RFID systems, and Internet of Things (IoT). He is a member of the IEEE and ACM.

▷ **For more information on this or any other computing topic, please visit our Digital Library at** www.computer.org/csdl.